

# Engineering unique localization transition with coupled Hatano-Nelson chains

Ritaban Samanta<sup>1\*</sup>, Aditi Chakrabarty<sup>1†</sup> and Sanjoy Datta<sup>1‡</sup>

<sup>1</sup> Department of Physics and Astronomy, National Institute of Technology, Rourkela, Odisha-769008, India.

\* ritabansamanta28@gmail.com, † aditichakrabarty030@gmail.com, ‡ dattas@nitrkl.ac.in

## Abstract

The paradigmatic Hatano-Nelson (HN) Hamiltonian induces a delocalization-localization (DL) transition in a one-dimensional (1D) lattice with random disorder, in striking contrast to its Hermitian counterpart. The DL transition also persists in the presence of a quasiperiodic potential separating completely delocalized and localized eigenstates. In this study, we reveal that coupling two 1D quasiperiodic Hatano-Nelson (QHN) lattices significantly alters the nature of the DL transition and identify two critical points,  $V_{c1} < V_{c2}$ , when the nearest neighbors of the two 1D QHN lattices are cross-coupled with strong hopping amplitudes under periodic boundary conditions (PBC). Complete delocalization occurs below  $V_{c1}$  and the states are completely localized above  $V_{c2}$ , while two mobility edges symmetrically emerge about  $\text{Re}[E] = 0$  between  $V_{c1}$  and  $V_{c2}$ . Notably, under specific asymmetric cross-hopping amplitudes,  $V_{c1}$  approaches zero, resulting in localized states even for an infinitesimally weak potential. Remarkably, we also find that the mobility edges precisely divide the delocalized and localized states in equal proportions. We demonstrate a possible implementation of these findings in a coupled waveguided array which can be exploited to control and manipulate the light localization depending upon the hopping amplitude in the two QHN chains.

Copyright attribution to authors.

This work is a submission to SciPost Physics.

License information to appear upon publication.

Publication information to appear upon publication.

Received Date

Accepted Date

Published Date

1

## 2 Contents

3	<b>1 Introduction</b>	2
4	<b>2 Model and methods</b>	3
5	2.1 The coupled QHN Hamiltonian	3
6	2.2 Delocalization-localization (DL) transition: the IPR	4
7	<b>3 Analytical understanding of the localization transition</b>	4
8	<b>4 Numerical Results and Discussions</b>	6
9	<b>5 Possible Experimental Implementation in Coupled Waveguides</b>	7
10	<b>6 Conclusions</b>	9

11	<b>7 Acknowledgements</b>	<b>9</b>
12	<b>References</b>	<b>10</b>

---

13  
14

## 15 **1 Introduction**

16 The concept of localization of the matter waves was laid down by P.W. Anderson in 1958,  
17 wherein the investigation revealed that in the presence of a sufficiently strong random disorder  
18 in the 3D lattice, the electronic conductivity ceases, hence becoming an insulator (frequently  
19 termed as the *Anderson* localization) [1]. The interesting features of Anderson localization  
20 has been implemented in many domains of physics, such as superconductors [2–4], photon-  
21 ics [5–8] and acoustics [9, 10]. However, it was later demonstrated using a scaling law that  
22 in the lattices of lower dimensions (1D/2D), even an infinitesimally small strength of the ran-  
23 dom disorder localizes all the electronic wave functions [11]. A few years later, in 1980, S.  
24 Aubry and G. André demonstrated that in quasiperiodic lattices, a delocalization-localization  
25 (DL) transition takes place even in lower dimensions [12, 13]. In the cosine-modulated Aubry-  
26 André-Harper (AAH) models, the DL transition occurs at a finite value of the quasiperiodic po-  
27 tential, governed by the self-duality of the Hamiltonian in the real and momentum spaces [14].  
28 For closed quantum systems which are described by Hermitian Hamiltonians, there have been  
29 many works based on the AAH model in the last few years [15–24]. Recently, such quasiperi-  
30 odic lattices have been realized in the ultracold atomic systems [25–27].

31 However, in reality, most of the condensed matter systems are coupled to the environment  
32 that exchanges either energy, or particles, or both with the surroundings. Such open systems  
33 are frequently mapped using a non-Hermitian Hamiltonian. Hatano and Nelson in 1996 intro-  
34 duced one such model which is an extension of the Anderson model with asymmetric hopping  
35 amplitudes. In his work, originally on the superconductors, it was shown that in the pres-  
36 ence of such random disorder, the DL transition is manifested in 1D systems. There have been  
37 many ongoing studies on the localization, spectral properties, self-duality and mobility edges  
38 in various non-Hermitian systems [17, 28–31]. Besides, such systems with asymmetric hop-  
39 ping amplitudes have been gaining attention over the years due to the phenomenon of skin  
40 effect wherein a macroscopic number of bulk states become localized at one of the edges under  
41 open boundaries [32–35].

42 On the other hand, some recent works have been carried out on coupled AAH chains in  
43 which two disparate chains of atoms are coupled to each other by some interchain hopping  
44 amplitudes [36, 37]. It was demonstrated that such a coupled Hermitian AAH chain shows  
45 interesting properties like the existence of mobility edges. However, to the best of our knowl-  
46 edge, the interplay of the quasiperiodicity and the coupling between the non-Hermitian chains  
47 of Hatano-Nelson(HN) type have not been investigated so far. Therefore, the aim of this work  
48 is to investigate a coupled HN bipartite chain in the presence of AAH type potential to closely  
49 scrutinize the localization behavior in such coupled systems and engineer unique localization  
50 features owing to the combined effect of the strength of the intra/inter chain coupling and the  
51 quasiperiodic potential. Intriguingly, we find that the presence of a strong interchain coupling  
52 between two dissimilar atoms in the two sublattices possessing symmetric and asymmetric in-  
53 terchain hopping between two atoms of adjacent unit cells render equal proportion of localized  
54 and delocalized states in the presence of quasiperiodic potential. Moreover, we find that in the  
55 latter case, half of the states are localized even for a very weak strength of the quasiperiodic  
56 potential, akin to the study by Anderson on 1D systems. We reveal that the coupling renders

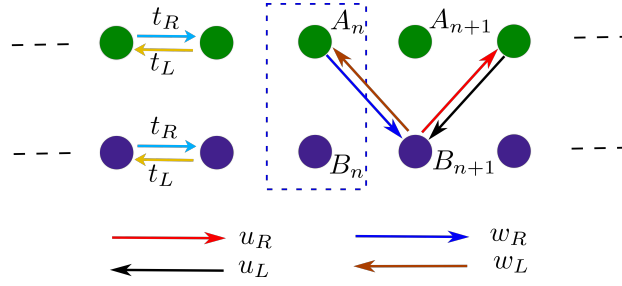


Figure 1: Schematic diagram of the coupled QHN model. Atoms A are depicted in blue and atoms B are depicted in green. The  $n$ th unit cell containing the two atoms is demonstrated by the dashed rectangle. The different interchain hopping amplitudes are mentioned below and are represented by coloured arrow lines.

57 distinct properties in the skin effect as compared to the conventional HN systems, wherein  
 58 some of the localized states (in the bulk) under PBC become skin-states under the OBC. Fi-  
 59 nally, we suggest a possible experimental set-up in coupled optical waveguides to exploit the  
 60 uniqueness of the localization of eigenstates at arbitrarily small strength in the quasiperiodic  
 61 potential.

62 This work is organized as follows: In Sec. 2.1, we discuss the coupled QHN Hamiltonian and  
 63 elaborate the method to numerically identify the delocalized and localized phases in Sec. 2.2.  
 64 We analytically determine the strength of the quasiperiodic potential ( $V_{c1}$  and  $V_{c2}$ ) where the  
 65 localization transitions occur in Sec. 3. In Sec. 4, we demonstrate our unique findings in the  
 66 presence of various ratios of the strong interchain coupling between the two QHN chains. We  
 67 propose a feasible experimental set-up in coupled optical waveguides in Sec. 5. Finally, Sec. 6  
 68 consists of a summary of the work, highlighting the important results and unique findings.

## 69 2 Model and methods

### 70 2.1 The coupled QHN Hamiltonian

71 We consider two uni-directional HN chains with quasiperiodic potential (consisting of two  
 72 sublattices A and B in a single unit cell) coupled to each other *via* an interchain hopping,  
 73 which we call a coupled quasiperiodic HN (QHN) Hamiltonian from here on.

74 The Hamiltonian in such a coupled system is given by,

$$\mathcal{H} = \mathcal{H}_A + \mathcal{H}_B + \mathcal{H}_C, \quad (1)$$

75 where,  $\mathcal{H}_A$  ( $\mathcal{H}_B$ ) is the Hamiltonian for chain 1 (2) of atom A (B) and  $\mathcal{H}_C$  introduces the inter-  
 76 chain coupling between chains 1 and 2. The individual terms of the Hamiltonian are described  
 77 as,

$$\begin{aligned} \mathcal{H}_{A(B)} = & \sum_{n=1}^{N-1} \left( t_R c_{n+1,A(B)}^\dagger c_{n,A(B)} + t_L c_{n,A(B)}^\dagger c_{n+1,A(B)} \right) \\ & + \sum_{n=1}^N V \cos(2\pi n \alpha) c_{n,A(B)}^\dagger c_{n,A(B)}. \end{aligned} \quad (2)$$

78 Here,  $c_{n,x}^\dagger$  ( $c_{n,x}$ ) are the fermionic creation (annihilation) operators at the site  $n$  of sub-  
 79 lattice  $x = A(B)$ . The first two terms of the Hamiltonian  $\mathcal{H}_{A(B)}$  define the usual asymmetric  
 80 intrachain hopping of the fermions between the nearest neighbour sites in sublattices  $A(B)$  and

81 the second term is the onsite quasiperiodic potential.  $\alpha$  is an irrational number approximated  
 82 as  $F_{n-1}/F_n$ , where  $F_n$  and  $F_{n-1}$  are the  $n$ th and  $(n-1)$ th terms of the Fibonacci series respec-  
 83 tively. Throughout this work, we have considered  $\alpha$  to be  $(\sqrt{5}-1)/2$  which approximates the  
 84 inverse golden mean ratio. The final part of the Hamiltonian which couples the two distinct  
 85 HN chains *via*. interchain coupling amplitudes is given as,

$$\mathcal{H}_C = \sum_{n=1}^N \left( u_R c_{n+1,A}^\dagger c_{n,B} + u_L c_{n,B}^\dagger c_{n+1,A} + w_R c_{n+1,B}^\dagger c_{n,A} + w_L c_{n,A}^\dagger c_{n+1,B} \right). \quad (3)$$

86 The interchain coupling  $u_R(u_L)$  is the hopping strength from  $B_n \rightarrow A_{n+1}(A_{n+1} \rightarrow B_n)$ ,  
 87 whereas  $w_R(w_L)$  is the hopping strength of  $A_n \rightarrow B_{n+1}(B_{n+1} \rightarrow A_n)$ . All these terms of the  
 88 inter and intra chain coupling are depicted in a schematic in Fig. 1.

## 89 2.2 Delocalization-localization (DL) transition: the IPR

90 The localized and delocalized behaviour of the eigenstates of the system is characterised by  
 91 estimating the value of the Inverse Participation Ratio (IPR). The IPR for a given eigenstate  
 92 ( $m$ ) is given by [38],

$$IPR_m = \frac{\sum_{n=1}^N \sum_{x=A,B} |\psi_{n,x}^m|^4}{\left( \sum_{n=1}^N \sum_{x=A,B} |\psi_{n,x}^m|^2 \right)^2} \quad (4)$$

93 where,  $\psi_{n,x}^m$  is the normalized wave function of eigenstate labelled by  $m$  at site  $n$  for the  
 94 chain  $x = A, B$ . Here,  $N$  is the size of the system and the number of total eigenstates is given  
 95 by  $L = 2N$ . It is well known that for the delocalized states, the  $IPR$  varies as  $IPR \sim L^{-1}$ . In the  
 96 thermodynamic limit ( $N \rightarrow \infty$ ), and therefore  $IPR \sim 0$ . In contrast, for the localized states,  
 97 the  $IPR$  is independent of the system size and approaches 1 in the thermodynamic limit. All  
 98 our numerical estimates are for a lattice with 610 sites, unless specifically mentioned.

## 99 3 Analytical understanding of the localization transition

100 In the following discussion, we analytically estimate the critical value of quasiperiodic potential  
 101 for the DL transition in the coupled QHN Hamiltonian as defined in Sec. 2.1. The Hamiltonian  
 102 consists of creation and annihilation operators of two sublattices, which can be effectively  
 103 combined into a single equation in terms of a spinor representation [39] given as,

$$b = \begin{pmatrix} c_A \\ c_B \end{pmatrix} \quad (5)$$

104 Using Eq. (5), one can immediately obtain,

$$\mathcal{H} = \sum_{n=1}^N \left( b_n^\dagger T_1 b_{n+1} + b_{n+1}^\dagger T_2 b_n \right) + \sum_{n=1}^N b_n^\dagger \epsilon(n) b_n, \quad (6)$$

105 where,

$$\epsilon(n) = \begin{pmatrix} V_n & 0 \\ 0 & V_n \end{pmatrix} \quad (7)$$

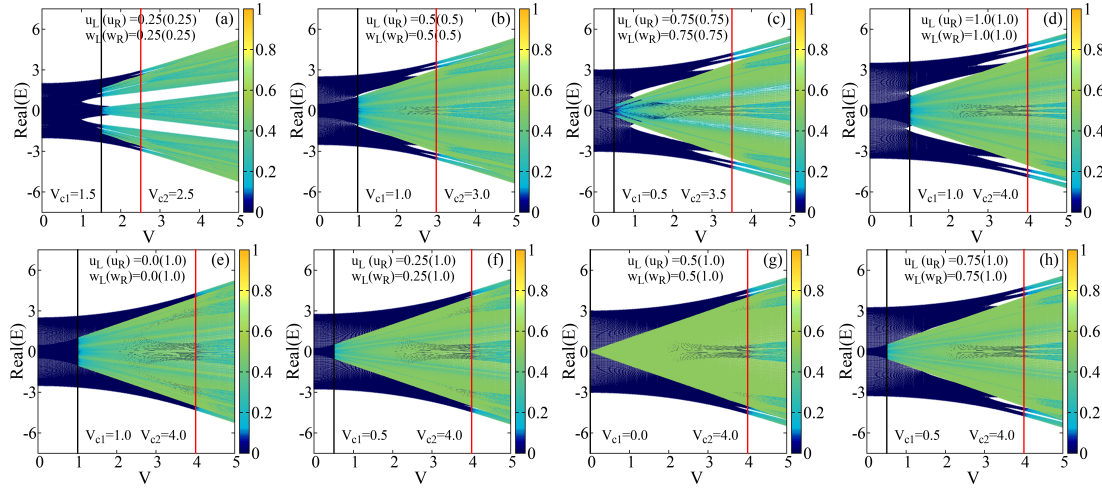


Figure 2: The localization behavior in a strongly coupled QHN Hamiltonian with  $t_L = 0.5, t_R = 1.0$  in a lattice with  $N = 610$  sites under PBC with interchain hopping between the two adjacent unit cells. Projection of IPR as a function of the real part of the eigen-energy and quasiperiodic potential ( $V$ ) for (a-d) symmetric interchain hopping and (e-h) asymmetric interchain hopping. In both the panels, the DL transition is shown as a dark blue to green transition. In particular, the parameters of interchain coupling are: (a)  $u_L = u_R = w_L = w_R = 0.25$ , (b)  $u_L = u_R = w_L = w_R = 0.5$ , (c)  $u_L = u_R = w_L = w_R = 0.75$ , (d)  $u_L = u_R = w_L = w_R = 1.0$ , (e)  $u_L = w_L = 0.0$  and  $u_R = w_R = 1.0$ , (f)  $u_L = w_L = 0.25$  and  $u_R = w_R = 1.0$ , (g)  $u_L = w_L = 0.5$  and  $u_R = w_R = 1.0$  (h)  $u_L = w_L = 0.75$  and  $u_R = w_R = 1.0$ .

106 and

$$T_1 = \begin{pmatrix} t_L & w_L \\ u_L & t_L \end{pmatrix}; T_2 = \begin{pmatrix} t_R & u_R \\ w_R & t_R \end{pmatrix}. \quad (8)$$

107 We introduce the wave function as,

$$\psi_n^m = \begin{pmatrix} \psi_{n,A}^m \\ \psi_{n,B}^m \end{pmatrix}, \quad (9)$$

108 where,  $\psi_{n,x}^m$  is the normalized wave function of eigenstate labelled by  $m$  at site  $n$  for the chain  
109  $x = A, B$ . Substituting Eq. (9) in Eq. (6), we obtain,

$$(E_m \mathbb{1} - \epsilon(n))\psi_n^m = T_1 \psi_{n+1}^m + T_2 \psi_{n-1}^m \quad (10)$$

110 Eq. (10) can be disintegrated into the following coupled equations:

$$\begin{aligned} (E_m - V_n)\psi_{n,A}^m &= t_L \psi_{n+1,A}^m + \\ t_R \psi_{n-1,A}^m &+ w_L \psi_{n+1,B}^m + u_R \psi_{n-1,B}^m, \end{aligned} \quad (11)$$

111 and

$$\begin{aligned} (E_m - V_n)\psi_{n,B}^m &= t_L \psi_{n+1,B}^m + \\ t_R \psi_{n-1,B}^m &+ w_R \psi_{n-1,A}^m + u_L \psi_{n+1,A}^m. \end{aligned} \quad (12)$$

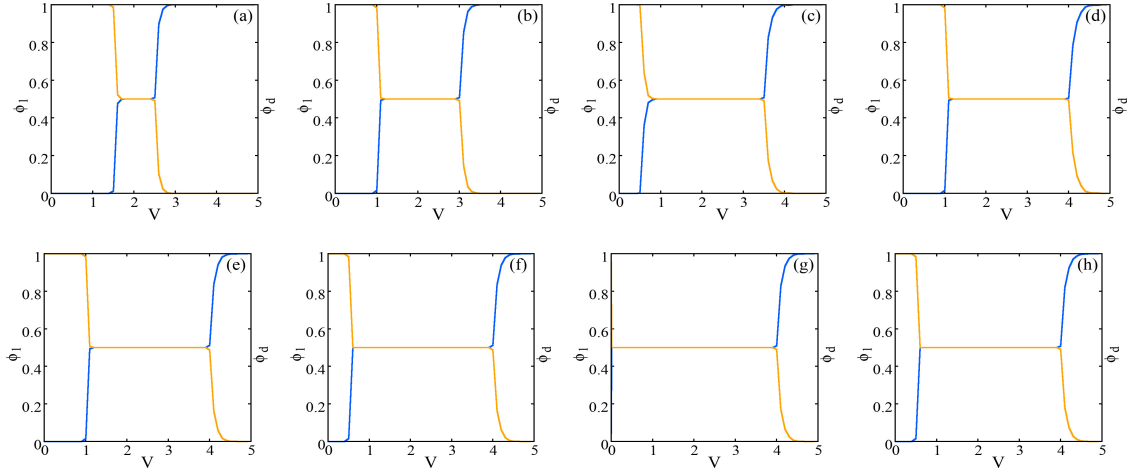


Figure 3: The fraction of localized states ( $\phi_l$ ) in blue and delocalized states ( $\phi_d$ ) in yellow corresponding to the parameters of Fig 2. States with  $IPR \gtrsim 0.1$  was considered localized, otherwise the states are considered to be delocalized in nature.

112 Applying the following canonical transformation

$$\psi_n^{m\pm} = \frac{\psi_{n,A}^m \pm \psi_{n,B}^m}{\sqrt{2}} \quad (13)$$

113 and with the following restrictions, i.e.,  $u_R = w_R = u_1$  and  $u_L = w_L = u_2$ , the system can be  
114 exactly mapped to two uncoupled QHN chains. This can be explicitly written as,

$$(E_m - V_n)\psi_n^{m+} = (t_L + u_2)\psi_{n+1}^{m+} + (t_R + u_1)\psi_{n-1}^{m+} \quad (14)$$

115 and

$$(E_m - V_n)\psi_n^{m-} = (t_L - u_2)\psi_{n+1}^{m-} + (t_R - u_1)\psi_{n-1}^{m-} \quad (15)$$

116 The full spectrum is therefore composed of the spectra of the two uncoupled QHN chains,  
117 i.e.,  $E_m^- = E_m - V_n$  and  $E_m^+ = E_m - V_n$ , which are identical. From Eqs. 14 and 15, one expects  
118 two localization transitions at two critical strengths of the quasiperiodic potential at [40],

$$V_{c1} = 2\left[\max(|t_L - u_2|, |t_R - u_1|)\right], \quad (16)$$

119 and

$$V_{c2} = 2\left[\max(|t_L + u_2|, |t_R + u_1|)\right]. \quad (17)$$

120  $V_{c1}$  provides the maximum value of quasiperiodic potential below which all the eigenstates  
121 are delocalized.  $V_{c2}$  is that strength of the potential above which all the states become com-  
122 pletely localized. It is interesting to note that one can engineer a system where  $V_{c1}$  is zero,  
123 when the conditions  $|t_L - u_2| = 0$  and  $|t_R - u_1| = 0$  are simultaneously satisfied.

## 124 4 Numerical Results and Discussions

125 In this section, we analyse the phase diagram of the DL transition in the presence of a strong  
126 interchain coupling between the two QHN chains A and B. The ratio of intrachain hopping  
127 strengths of the chains A(B) is  $t_L/t_R = 0.5$ . In the upper panel of Fig. 2, we consider the case

128 of symmetric interchain coupling. It is clear from Figs. 2(a)-(d) that the DL transition does  
 129 not occur at  $V_c = 2\max[J_R, J_L]$  (which is the critical value of DL transition in QHN chain). It  
 130 is clearly visible that all the eigenstates are perfectly delocalized for  $V \lesssim V_{c1}$  and localized for  
 131  $V \gtrsim V_{c2}$ . The value of  $V_{c1}$  and  $V_{c2}$  as determined in Eqs. (16) and (17) agrees excellently with  
 132 all the numerical estimates. Furthermore, as is evident, the eigenstates between these two  
 133 critical points are a mixture of both the delocalized and localized states, separated at a critical  
 134 energy, termed as the mobility edge.

135 Next, we consider the case when the interchain coupling is asymmetric in nature in the  
 136 lower panel of Fig. 2. It is clear that the localization behavior drastically changes upon consid-  
 137 ering a particular strength of asymmetry, i.e, say,  $u_L = 0.5$ ,  $u_R = 1.0$  and  $w_L = 0.5$ ,  $w_R = 1.0$ .  
 138 Such a tendency of  $V_{c1}$  approaching 0 is expected when  $|t_L - u_2|$  and  $|t_R - u_1|$  are both zero, as  
 139 already explained. This particular case is of interest since the localized states appear even for a  
 140 low value of the quasiperiodic potential, similar to the 1D original Anderson model, although  
 141 in this case not all the states are localized.

142 To have a closer look into the nature of states in between  $V_{c1}$  and  $V_{c2}$ , we check the frac-  
 143 tion of localized ( $\phi_l$ ) and delocalized states ( $\phi_d$ ). We consider the states with  $IPR \gtrsim 0.1$  as  
 144 being absolutely localized, and below the limit the states are considered to be delocalized. We  
 145 examine these different regions separately by plotting the fraction of localized and delocalized  
 146 states as a function of the quasiperiodic potential corresponding to the parameters of Figs. 2.  
 147 From Figs. 3(a-h), we can easily infer that there is a co-existence of localized and delocalized  
 148 states for a wide regime in the quasiperiodic potential. Moreover, interestingly 50% of these  
 149 states are delocalized while the remaining states are localized. This proportionate behaviour is  
 150 consistent throughout the entire intermediate region. Furthermore, it is also important to see  
 151 that in the case where  $V_{c1} = 0$ , exactly 50% localized states appear at even a tiny quasiperiodic  
 152 potential, as previously discussed.

153 As already elucidated, Fig. 2(g) gives rise to an interesting outcome of localization at a very  
 154 minute value of the quasiperiodic potential  $V$ . Therefore, in order to understand whether the  
 155 same behavior is retained under the OBC, we plot the phase diagram in Fig. 4(a). However,  
 156 from Fig 4(b), we can infer that proportion of delocalized and localized states does not remain  
 157 same (i.e., at 50%) when the boundaries are open. It is clear, that the localized wavefunctions  
 158 under PBC become delocalized(skin modes under the OBC) since  $\phi_d$  increases. From Fig. 4(a-  
 159 i) (state picked up from the dark blue regime of the phase diagram), it is clear that the state  
 160 becomes a skin state under OBC as expected. However, we have found out that the light blue  
 161 regime infact consists of both skin states (localized at right edge as demonstrated in Fig. 4(a-  
 162 ii)) and localized states (where the localization is not necessarily towards the right edge as  
 163 shown in Fig. 4(a-iii). This is in stark contrast to the 1D HN systems in the absence of the  
 164 coupling. One can therefore infer that additional skin modes are formed from the localized  
 165 states under OBC due to the coupling between such QHN chains, and hence the one-to-one  
 166 correspondence between the delocalized(skin) states under PBC(OBC) breaks down in the  
 167 presence of the coupling.

## 168 5 Possible Experimental Implementation in Coupled Waveguides

169 The equation of a coupled waveguide array at position  $n$  is written in the form,

$$-i \frac{d\psi_n}{dz} = J_L \psi_{n+1} + J_R \psi_{n-1} + V_n \psi_n \quad (18)$$

170 where  $J_L$  and  $J_R$  tune the spacing in between the waveguides, and is non-Hermitian in the  
 171 usual sense. Eq. 18 is an optical analogue of the Schrodinger equation where the time  $t$  is

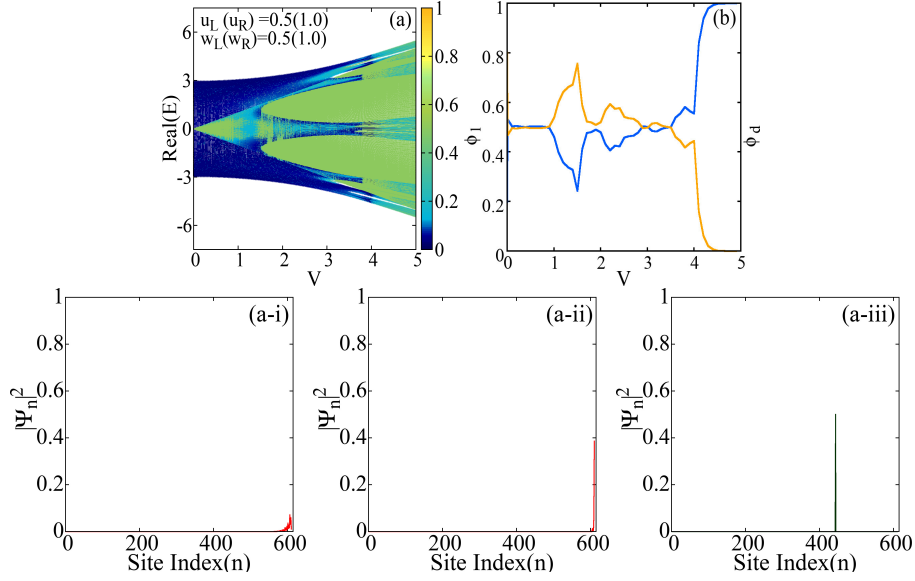


Figure 4: The localization behavior in a strongly coupled QHN Hamiltonian with  $t_L = 0.5$ ,  $t_R = 1.0$  for a lattice with  $N = 610$  sites under OBC with interchain hopping between the two adjacent unit cells. (a) Projection of *IPR* as a function of the real part of the eigen-energy and quasiperiodic potential ( $V$ ), where the DL transition is shown as a dark blue to green color transition. The other parameters of interchain coupling are: (a)  $u_L = 0.5$ ,  $u_R = 1.0$ ,  $w_L = 0.5$  and  $w_R = 1.0$ . (b) The fraction of localized states ( $\phi_l$ ) in blue and delocalized states ( $\phi_d$ ) in yellow, corresponding to the parameters of Fig 2. Figs. a(i-iii) in the lower panel demonstrates the behavior of the wavefunction probabilities at different lattice sites corresponding to the figure in the upper panel at  $V = 1.5$ . (a-i) skin modes (dark blue regime of *IPR*), (a-ii) skin modes in the light blue regime of *IPR*, and (a-iii) localized regime (in green regime of *IPR*).

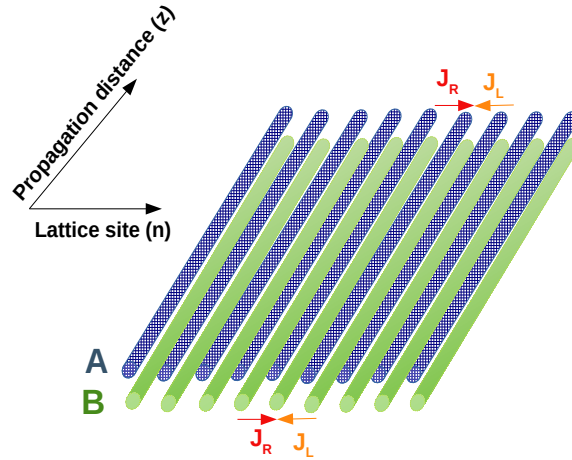


Figure 5: Schematic diagram of the coupled waveguide with asymmetric hopping. Atoms *A* and *B* which depict the waveguide channels in the optical set-up are depicted in blue and green respectively.



172 replaced by the spatial distance between the parallel waveguides  $z$ , due to the mathematical  
173 equivalence between the two [41, 42]. Since we have two atoms (A and B) in a unit cell, we  
174 can consider two layers of waveguided arrays (called coupled waveguided arrays) as depicted  
175 in the schematic given in Fig. 5. Such coupled waveguides have already been fabricated on a  
176 semiconducting AlGaAs substrate when  $J_L = J_R$  [42]. The array is composed of a core layer  
177 sandwiched between two cladding layers, where the upper cladding layer is etched quasiperi-  
178 odically, where one can modulate the width of the waveguides quasiperiodically to realize the  
179 quasiperiodic onsite potential. The etching makes the core beneath it have a lower effective  
180 refraction index, resulting in a array of coupled 1D waveguides. One can tune  $J_L$  and  $J_R$  using  
181 a beam-splitter. We consider another coupled waveguide placed exactly below it, which could  
182 mimic the coupled QHN system as discussed in our main text. Since our work demonstrates  
183 the avenue to tune the strengths of  $V_{c1}$  and  $V_{c2}$  to engineer the localization transitions, such a  
184 coupled waveguided array can prove to be a boon to experimentalists working in such optical  
185 set-ups.

## 186 6 Conclusions

187 To summarize, this work scrutinizes the different localization attributes in non-Hermitian cou-  
188 pled quasiperiodic chains. The nature of DL transition at a threshold of the quasiperiodic  
189 potential ( $V_c = 2$ ) for NH-AAH chains with parameters  $t_L = 0.5$  and  $t_R = 1.0$  is well-known.  
190 However, unlike the generic DL transition in NH-AAH chains, a strong coupling between the  
191 atoms of adjacent unit cells of the two HN chains possessing the same directionalities under  
192 PBC renders an intermediate region, wherein the eigenstates are a mixture of equal proportion  
193 of delocalized and localized states. Interestingly, for the counterpart with asymmetry with  
194 specific hopping amplitudes, this intermediate region appears even in the presence of very  
195 tiny quasiperiodic potential, where the localized and delocalized states coexist. In this case as  
196 well, the proportion of localized and delocalized states remains identical. Moreover, under an  
197 OBC, we find a mixture of skin states and localized states in a regime of the localized portion  
198 in the PBC phase diagram. This is in contrary to the conventional HN systems where the lo-  
199 calized states under OBC can either be skin modes or be completely localized and the usual  
200 PBC-OBC correspondence that leads the delocalized states to become skin states, keeping the  
201 localized states intact completely breaks down in the presence of the coupling. We believe that  
202 these rich phases due to the coupling in non-Hermitian systems can be utilised in experiments  
203 related to coupled waveguides.

## 204 7 Acknowledgements

205 The authors are thankful to the High Performance Computing (HPC) facilities of the National  
206 Institute of Technology (Rourkela).

207 **Funding information** A part of the computation was carried out in the cluster procured from  
208 SERB (DST), India (Grant No. EMR/2015/001227). A.C. acknowledges CSIR-HRDG, India,  
209 for providing financial support via File No.- 09/983(0047)/2020-EMR-I..

210 **References**

- 211 [1] P. W. Anderson, *Absence of diffusion in certain random lattices*, Phys. Rev. **109**, 1492  
212 (1958), doi:[10.1103/PhysRev.109.1492](https://doi.org/10.1103/PhysRev.109.1492).
- 213 [2] D. E. Katsanos, S. N. Evangelou and C. J. Lambert, *Superconductivity-induced anderson*  
214 *localization*, Phys. Rev. B **58**, 2442 (1998), doi:[10.1103/PhysRevB.58.2442](https://doi.org/10.1103/PhysRevB.58.2442).
- 215 [3] I. S. Burmistrov, I. V. Gornyi and A. D. Mirlin, *Enhancement of the critical tempera-*  
216 *ture of superconductors by anderson localization*, Phys. Rev. Lett. **108**, 017002 (2012),  
217 doi:[10.1103/PhysRevLett.108.017002](https://doi.org/10.1103/PhysRevLett.108.017002).
- 218 [4] P. W. Anderson, K. A. Muttalib and T. V. Ramakrishnan, *Theory of the "universal"*  
219 *degradation of  $t_c$  in high-temperature superconductors*, Phys. Rev. B **28**, 117 (1983),  
220 doi:[10.1103/PhysRevB.28.117](https://doi.org/10.1103/PhysRevB.28.117).
- 221 [5] A. K. Sarychev, V. A. Shubin and V. M. Shalaev, *Anderson localization of surface plas-*  
222 *mons and nonlinear optics of metal-dielectric composites*, Phys. Rev. B **60**, 16389 (1999),  
223 doi:[10.1103/PhysRevB.60.16389](https://doi.org/10.1103/PhysRevB.60.16389).
- 224 [6] Y. Lahini, A. Avidan, F. Pozzi, M. Sorel, R. Morandotti, D. N. Christodoulides and Y. Sil-  
225 berberg, *Anderson localization and nonlinearity in one-dimensional disordered photonic*  
226 *lattices*, Phys. Rev. Lett. **100**, 013906 (2008), doi:[10.1103/PhysRevLett.100.013906](https://doi.org/10.1103/PhysRevLett.100.013906).
- 227 [7] D. M. Jović, Y. S. Kivshar, C. Denz and M. R. Belić, *Anderson localization of light*  
228 *near boundaries of disordered photonic lattices*, Phys. Rev. A **83**, 033813 (2011),  
229 doi:[10.1103/PhysRevA.83.033813](https://doi.org/10.1103/PhysRevA.83.033813).
- 230 [8] Y. Qiao, F. Ye, Y. Zheng and X. Chen, *Cavity-enhanced second-harmonic gener-*  
231 *ation in strongly scattering nonlinear media*, Phys. Rev. A **99**, 043844 (2019),  
232 doi:[10.1103/PhysRevA.99.043844](https://doi.org/10.1103/PhysRevA.99.043844).
- 233 [9] C. A. Condat and T. R. Kirkpatrick, *Observability of acoustical and optical localization*,  
234 Phys. Rev. Lett. **58**, 226 (1987), doi:[10.1103/PhysRevLett.58.226](https://doi.org/10.1103/PhysRevLett.58.226).
- 235 [10] S. M. Cohen, J. Machta, T. R. Kirkpatrick and C. A. Condat, *Crossover in the an-*  
236 *derson transition: Acoustic localization with a flow*, Phys. Rev. Lett. **58**, 785 (1987),  
237 doi:[10.1103/PhysRevLett.58.785](https://doi.org/10.1103/PhysRevLett.58.785).
- 238 [11] E. Abrahams, P. W. Anderson, D. C. Licciardello and T. V. Ramakrishnan, *Scaling theory*  
239 *of localization: Absence of quantum diffusion in two dimensions*, Phys. Rev. Lett. **42**, 673  
240 (1979), doi:[10.1103/PhysRevLett.42.673](https://doi.org/10.1103/PhysRevLett.42.673).
- 241 [12] S. Aubry and G. André, *Analyticity breaking and anderson localization in incommensurate*  
242 *lattices*, Ann. Israel Phys. Soc **3**(133), 18 (1980).
- 243 [13] P. G. Harper, *Single band motion of conduction electrons in a uniform magnetic field*,  
244 Proceedings of the Physical Society. Section A **68**(10), 874 (1955), doi:[10.1088/0370-](https://doi.org/10.1088/0370-1298/68/10/304)  
245 [1298/68/10/304](https://doi.org/10.1088/0370-1298/68/10/304).
- 246 [14] S. Longhi, *Metal-insulator phase transition in a non-hermitian aubry-andré-harper model*,  
247 Phys. Rev. B **100**, 125157 (2019), doi:[10.1103/PhysRevB.100.125157](https://doi.org/10.1103/PhysRevB.100.125157).
- 248 [15] P. Tong, *Localization and mobility edges in one-dimensional deterministic potentials*, Phys.  
249 Rev. B **50**, 11318 (1994), doi:[10.1103/PhysRevB.50.11318](https://doi.org/10.1103/PhysRevB.50.11318).

- 250 [16] A. Ossipov, M. Weiss, T. Kottos and T. Geisel, *Quantum mechanical re-*  
251 *laxation of open quasiperiodic systems*, Phys. Rev. B **64**, 224210 (2001),  
252 doi:[10.1103/PhysRevB.64.224210](https://doi.org/10.1103/PhysRevB.64.224210).
- 253 [17] Y. Yoo, J. Lee and B. Swingle, *Nonequilibrium steady state phases of the*  
254 *interacting aubry-andré-harper model*, Phys. Rev. B **102**, 195142 (2020),  
255 doi:[10.1103/PhysRevB.102.195142](https://doi.org/10.1103/PhysRevB.102.195142).
- 256 [18] J. B. Sokoloff, *Band structure and localization in incommensurate lattice potentials*, Phys.  
257 Rev. B **23**, 6422 (1981), doi:[10.1103/PhysRevB.23.6422](https://doi.org/10.1103/PhysRevB.23.6422).
- 258 [19] J. Sokoloff, *Unusual band structure, wave functions and electrical conductance in crys-*  
259 *tals with incommensurate periodic potentials*, Physics Reports **126**(4), 189 (1985),  
260 doi:[10.1016/0370-1573\(85\)90088-2](https://doi.org/10.1016/0370-1573(85)90088-2).
- 261 [20] M. Kohmoto, *Metal-insulator transition and scaling for incommensurate systems*, Phys.  
262 Rev. Lett. **51**, 1198 (1983), doi:[10.1103/PhysRevLett.51.1198](https://doi.org/10.1103/PhysRevLett.51.1198).
- 263 [21] D. J. Thouless, *Bandwidths for a quasiperiodic tight-binding model*, Phys. Rev. B **28**, 4272  
264 (1983), doi:[10.1103/PhysRevB.28.4272](https://doi.org/10.1103/PhysRevB.28.4272).
- 265 [22] H. Hiramoto and M. Kohmoto, *Electronic spectral and wavefunction properties of one-*  
266 *dimensional quasiperiodic systems: A scaling approach*, International Journal of Modern  
267 Physics B **06**(03n04), 281 (1992), doi:[10.1142/S0217979292000153](https://doi.org/10.1142/S0217979292000153).
- 268 [23] B. Kramer and A. MacKinnon, *Localization: theory and experiment*, Reports on Progress  
269 in Physics **56**(12), 1469 (1993), doi:[10.1088/0034-4885/56/12/001](https://doi.org/10.1088/0034-4885/56/12/001).
- 270 [24] I. Chang, K. Ikezawa and M. Kohmoto, *Multifractal properties of the wave functions of the*  
271 *square-lattice tight-binding model with next-nearest-neighbor hopping in a magnetic field*,  
272 Phys. Rev. B **55**, 12971 (1997), doi:[10.1103/PhysRevB.55.12971](https://doi.org/10.1103/PhysRevB.55.12971).
- 273 [25] G. Roati, C. D'Errico, L. Fallani, M. Fattori, C. Fort, M. Zaccanti, G. Modugno, M. Mod-  
274 uugno and M. Inguscio, *Anderson localization of a non-interacting bose-einstein condensate*,  
275 Nature **453**(7197), 895 (2008), doi:[10.1038/nature07071](https://doi.org/10.1038/nature07071).
- 276 [26] B. Deissler, M. Zaccanti, G. Roati, C. D'Errico, M. Fattori, M. Modugno, G. Modugno and  
277 M. Inguscio, *Delocalization of a disordered bosonic system by repulsive interactions*, Nature  
278 physics **6**(5), 354 (2010), doi:[10.1038/nphys1635](https://doi.org/10.1038/nphys1635).
- 279 [27] M. Schreiber, S. S. Hodgman, P. Bordia, H. P. Lüschen, M. H. Fischer, R. Vosk, E. Alt-  
280 man, U. Schneider and I. Bloch, *Observation of many-body localization of inter-*  
281 *acting fermions in a quasirandom optical lattice*, Science **349**(6250), 842 (2015),  
282 doi:[10.1126/science.aaa7432](https://doi.org/10.1126/science.aaa7432).
- 283 [28] L.-Z. Tang, G.-Q. Zhang, L.-F. Zhang and D.-W. Zhang, *Localization and topological*  
284 *transitions in non-hermitian quasiperiodic lattices*, Phys. Rev. A **103**, 033325 (2021),  
285 doi:[10.1103/PhysRevA.103.033325](https://doi.org/10.1103/PhysRevA.103.033325).
- 286 [29] A. F. Tzortzakakis, K. G. Makris, A. Szameit and E. N. Economou, *Transport and*  
287 *spectral features in non-hermitian open systems*, Phys. Rev. Res. **3**, 013208 (2021),  
288 doi:[10.1103/PhysRevResearch.3.013208](https://doi.org/10.1103/PhysRevResearch.3.013208).
- 289 [30] Q.-B. Zeng, S. Chen and R. Lü, *Anderson localization in the non-hermitian aubry-*  
290 *andré-harper model with physical gain and loss*, Phys. Rev. A **95**, 062118 (2017),  
291 doi:[10.1103/PhysRevA.95.062118](https://doi.org/10.1103/PhysRevA.95.062118).

- 292 [31] L.-J. Zhai, S. Yin and G.-Y. Huang, *Many-body localization in a non-hermitian quasiperiodic*  
293 *system*, Phys. Rev. B **102**, 064206 (2020), doi:[10.1103/PhysRevB.102.064206](https://doi.org/10.1103/PhysRevB.102.064206).
- 294 [32] S. Yao and Z. Wang, *Edge states and topological invariants of non-hermitian systems*, Phys.  
295 *Rev. Lett.* **121**, 086803 (2018), doi:[10.1103/PhysRevLett.121.086803](https://doi.org/10.1103/PhysRevLett.121.086803).
- 296 [33] T. E. Lee, *Anomalous edge state in a non-hermitian lattice*, Phys. Rev. Lett. **116**, 133903  
297 (2016), doi:[10.1103/PhysRevLett.116.133903](https://doi.org/10.1103/PhysRevLett.116.133903).
- 298 [34] V. M. Martinez Alvarez, J. E. Barrios Vargas and L. E. F. Foa Torres, *Non-hermitian ro-*  
299 *burst edge states in one dimension: Anomalous localization and eigenspace condensation at*  
300 *exceptional points*, Phys. Rev. B **97**, 121401 (2018), doi:[10.1103/PhysRevB.97.121401](https://doi.org/10.1103/PhysRevB.97.121401).
- 301 [35] C. H. Lee, L. Li and J. Gong, *Hybrid higher-order skin-topological modes in nonreciprocal*  
302 *systems*, Phys. Rev. Lett. **123**, 016805 (2019), doi:[10.1103/PhysRevLett.123.016805](https://doi.org/10.1103/PhysRevLett.123.016805).
- 303 [36] S. Mu, L. Zhou, L. Li and J. Gong, *Non-hermitian pseudo mobility edge in a coupled chain*  
304 *system*, Phys. Rev. B **105**, 205402 (2022), doi:[10.1103/PhysRevB.105.205402](https://doi.org/10.1103/PhysRevB.105.205402).
- 305 [37] M. Rossignolo and L. Dell'Anna, *Localization transitions and mobility edges in coupled*  
306 *aubry-andré chains*, Phys. Rev. B **99**, 054211 (2019), doi:[10.1103/PhysRevB.99.054211](https://doi.org/10.1103/PhysRevB.99.054211).
- 307 [38] S. Roy, S. Chattopadhyay, T. Mishra and S. Basu, *Critical analysis of the reentrant local-*  
308 *ization transition in a one-dimensional dimerized quasiperiodic lattice*, Phys. Rev. B **105**,  
309 214203 (2022), doi:[10.1103/PhysRevB.105.214203](https://doi.org/10.1103/PhysRevB.105.214203).
- 310 [39] M. Rossignolo and L. Dell'Anna, *Localization transitions and mobility edges in coupled*  
311 *aubry-andré chains*, Phys. Rev. B **99**, 054211 (2019), doi:[10.1103/PhysRevB.99.054211](https://doi.org/10.1103/PhysRevB.99.054211).
- 312 [40] H. Jiang, L.-J. Lang, C. Yang, S.-L. Zhu and S. Chen, *Interplay of non-hermitian skin*  
313 *effects and anderson localization in nonreciprocal quasiperiodic lattices*, Phys. Rev. B **100**,  
314 054301 (2019), doi:[10.1103/PhysRevB.100.054301](https://doi.org/10.1103/PhysRevB.100.054301).
- 315 [41] E. T. Kokkinakis, K. G. Makris and E. N. Economou, *Anderson localization versus hopping*  
316 *asymmetry in a disordered lattice*, arXiv (2024), doi:[10.48550/arXiv.2407.10746](https://doi.org/10.48550/arXiv.2407.10746).
- 317 [42] Y. E. Kraus, Y. Lahini, Z. Ringel, M. Verbin and O. Zilberberg, *Topological states*  
318 *and adiabatic pumping in quasicrystals*, Phys. Rev. Lett. **109**, 106402 (2012),  
319 doi:[10.1103/PhysRevLett.109.106402](https://doi.org/10.1103/PhysRevLett.109.106402).